Dynamic stability of parametrically-excited linear resonant beams under periodic axial force*

Li Jing(李 晶)[a)b)c)d)], Fan Shang-Chun(樊尚春)[a)b)c)],
Li Yan(李 艳)[a)b)c)†], and Guo Zhan-She(郭占社)[a)b)c)]

[a)] *School of Instrument Science & Opto-electronics Engineering, Beihang University, Beijing* 100191, *China*
[b)] *Key Laboratory of Precision Opto-mechatronics Techonology, Ministry of Education Beijing* 100191, *China*
[c)] *Key Laboratory of Inertial Science and Technology for National Defence, Beijing* 100191, *China*
[d)] *School of Information and Communication Engineering, North University of China, Taiyuan* 030051, *China*

(Received 7 March 2012; revised manuscript received 7 July 2012)

The parametric dynamic stability of resonant beams with various parameters under periodic axial force is studied. It is assumed that the theoretical formulations are based on Euler–Bernoulli beam theory. The governing equations of motion are derived by using the Rayleigh–Ritz method and transformed into Mathieu equations, which are formed to determine the stability criterion and stability regions for parametrically-excited linear resonant beams. An improved stability criterion is obtained using periodic Lyapunov functions. The boundary points on the stable regions are determined by using a small parameter perturbation method. Numerical results and discussion are presented to highlight the effects of beam length, axial force and damped coefficient on the stability criterion and stability regions. While some stability rules are easy to anticipate, we draw some conclusions: with the increase of damped coefficient, stable regions arise; with the decrease of beam length, the conditions of the damped coefficient arise instead. These conclusions can provide a reference for the robust design of parametrically-excited linear resonant sensors.

Keywords: resonant beams, dynamic stability, parametrical excitation, periodic axial force

PACS: 04.40.Dg, 02.30.Hq, 05.10.–a **DOI:** 10.1088/1674-1056/21/11/110401

1. Introduction

Resonance is a property of a system that describes an enhanced response at a certain characteristic natural frequency which is wholly determined by parameters of the system.[1] At this special frequency, the system retains the input energy with minimum loss. At a microscopic scale, operating systems at resonance enhance the effects of small forces and a device's signal-to-noise ratio. Operation at resonance is not only advantageous for micromechanical actuators but also for sensing. Resonant sensing often involves the detection of an input measurand by means of resonant frequency shift in the sensing device. In applications such as resonant sensors, large amplitude motion is necessary, and operation at resonance is highly desirable. The resonator sensor element is often built into a larger device that transmits the effect of the parameter to be measured as a variation in the spring constant of the resonant sensor element. Actually, most of the resonant sensor elements are resonant beams, which are the most important part of the resonant sensor. Resonant sensors have attracted increasing research efforts and are regarded as one of the most promising candidates for future advanced composites in many engineering sectors such as the aerospace, aircraft, automobile, and defense industries.

Numerous studies on the dynamic behavior of resonant beam structures have been reported. Based on the Euler–Bernoulli beam theory, the effects of the resonant frequencies and mode shapes of the resonant beams have been studied.[2−6] The effect of periodic axial force on the vibration frequency and stability of resonant beams has been investigated by many scientists and engineers.[7−11] It is known that parametric excitation occurs when system parameter stiffness varies with time. Periodic axial force changes structural stiffness, and hence produces parametric excitation. The parametrically-excited structure is gov-

*Project supported by the National Natural Science Foundation of China (Grant No. 60927005), the 2012 Innovation Foundation of BUAA for PhD Graduates, and the Fundamental Research Funds for the Central Universities, China (Grant No. YWF-10-01-A17).
†Corresponding author. E-mail: yanli.83@163.com
© 2012 Chinese Physical Society and IOP Publishing Ltd

erned by the Mathieu equation, if the axial excitation is harmonic. The archetypal equation for this Mathieu equation is

$$q''(z) + (\delta + \varepsilon \cos 2z)\, q(z) = 0. \tag{1}$$

When applying in the analysis of the beam, $q(z)$ responses for vibratory tracking with time, the parameter δ represents the natural resonant frequency of a resonant beam. The significant perturbation term $\varepsilon \cos 2z$ represents the modulation of the stiffness of the resonant beam at the periodic axial force frequency. This equation, though linear, is quite complicated due to its explicit time dependence and hence the absence of closed-form solutions. Instead, the common method of attack is to consider the stability of the origin, which exactly represents the stability of the resonant beams. Hence, it is helpful to study the stability of resonant beams using the Mathieu equation.

The Mathieu equation is an excellent paradigm to study parametric (subharmonic) resonance. Recently, the stability of the Mathieu equation has been studied using the Floquet theory.[12−16] The parameter space (δ, ε) was divided into regions of stability and instability in Refs. [17]–[19]. Arrowsmith *et al.*[20] dealt with how the size of the parametric regions of stability for the Mathieu equation can be enlarged. There are many extensions to this equation. Younesian *et al.*[21] considered a cubic order with two small parameters and terms in sin and cos, but the extension to the Mathieu equation is nonlinear. The stability of a quasi-periodic nonlinear Mathieu equation has also been analyzed,[22−26] but the extensions to the Mathieu equation contain two periodic terms in different frequencies.

With the addition of a damping term $\mu q'(z)$, Eq. (1) becomes

$$q''(z) + \mu q'(z) + (\delta + \varepsilon \cos 2z)\, q(z) = 0, \tag{2}$$

where μ is the damped coefficient. This equation holds true under the condition that the resonant beams do not vibrate at resonant frequency, but the condition of the driving force is not equal to the damped force. This situation occurs in a wide variety of practical problems. In Ref. [27], it is shown that the elastic motion of a large space structure, which is modeled as a non-spinning, axisymmetric beam undergoing flexural vibrations, is governed by the damped Mathieu equation.

Using frequency domain stability criteria, Taylor and Narendra[28] derived three sufficient conditions for the stability of Eq. (2). However, all of the three results were derived under the restrictive assumption. Based on the notion of kinematic similarity and an estimate of the growth rate of solutions, Gunderson *et al.*[29] relaxed this assumption and derived two sufficient conditions for the stability of Eq. (2). Based on an earlier contribution of Pipes,[30] Richards[31−33] suggested the replacement of the time-varying term of Eq. (2) by a trapezoidal function, thereby converting it into Hill's equation, which admits a closed form solution. It provided an excellent approximation to the lossless Mathieu equation.

All of the above-mentioned studies about the Mathieu equation are just mathematical analysis, and do not have any physical instruments. However, the methods used are not applicable in analyzing the dynamic stability of resonant beams.

The objective of this paper is to investigate the dynamic parametric stability of resonant beams under periodic axial force by using the Mathieu equation. First of all, the parametric resonant characteristics based on resonant beams are introduced, and the physical relativity between the Mathieu equation and parametrical resonant beams are studied. Then, a dynamic stability index is devised and utilized to study the influence of various parameters on the dynamic stability. The effects of beam length, axial force, and damped coefficient on the stability criterion and stability regions are investigated and discussed.

2. Mathematical modeling

2.1. Free vibration

The vibration equations of motion for a resonant beam subjected to periodic axial force are established by applying the Lagrange method. The derivation of these equations is based on the assumptions that the resonant beams are Euler–Bernoulli beams. Figure 1 shows a typical resonant beam of length L, width b, and thickness h. The beam is in the clamped–clamped end condition and exposed under periodic axial force $F = F_0 \cos \omega_{\mathrm{d}} t$. The axial forces are positive for compressive and negative for tensile.

We denote the Young's modulus by E, beam mass density by ρ, the moment of inertia by I, damped coefficient by ξ, and the longitudinal displacement by $y(x, t)$.

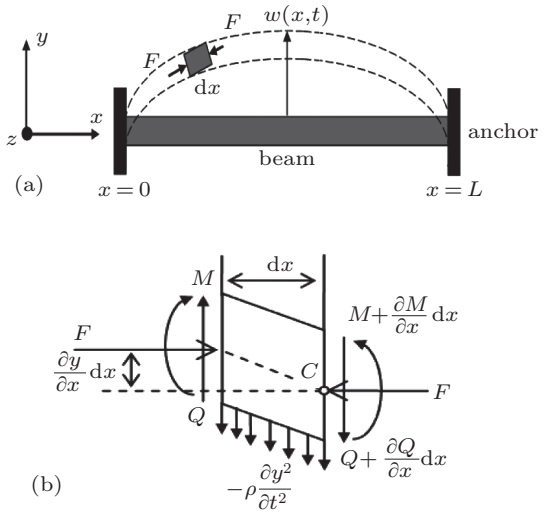


Fig. 1. (a) Beam configuration and (b) coordinate system.

The equation of motion ($w(x,t) = y(x,t) = \phi(x)q(t)$) governs the transverse vibration as a function of the position x along the length of the beam and time$t$. The $\phi(x)$ is mode-shape function, and $q(t)$ responses for vibratory tracking with time. The free vibratory equation is expressed as follows:

$$\int_0^L \rho A\phi^2 \,\mathrm{d}x\ddot{q} + \int_0^L \xi\phi^2 \,\mathrm{d}x\dot{q} + \left(\int_0^L EI\left(\frac{\partial^2\phi}{\partial x^2}\right)^2 \mathrm{d}x + \int_0^L F\left(\frac{\partial\phi}{\partial x}\right)^2 \mathrm{d}x\right)q = 0. \tag{3}$$

According to the Lagrange-energy method, the result equation is obtained as follows:

$$M_{\text{eff}}\ddot{q} + B_{\text{eff}}\dot{q} + K_{\text{eff}}q = 0, \tag{4}$$

where M_{eff}, K_{eff}, and B_{eff} is the mass, stiffness, and damping matrix, respectively. According to the Rayleigh–Ritz method, boundary conditions are given by

$$w(0) = w(L) = 0, \quad \left.\frac{\mathrm{d}w}{\mathrm{d}x}\right|_{x=0} = \left.\frac{\mathrm{d}w}{\mathrm{d}x}\right|_{x=L} = 0.$$

The resonant beams are working in the first mode. Using this convention, the natural frequency ω_n and the no-load natural frequency ω_0 of the resonant beam are obtained as follows:

$$\omega_{\text{n}} = \sqrt{\frac{K_{\text{eff}}}{M_{\text{eff}}}} = \sqrt{\left[\int_0^1 \frac{EI}{L^3}\left(\frac{\partial^2\phi}{\partial\tau^2}\right)^2 \mathrm{d}\tau + \int_0^1 \frac{F}{L}\left(\frac{\partial\phi}{\partial\tau}\right)^2 \mathrm{d}\tau\right] \Big/ \int_0^1 \rho AL\phi^2 \,\mathrm{d}\tau} = \omega_0\sqrt{1 + \frac{0.293FL^2}{12EI}}, \tag{5}$$

$$\omega_0 = \sqrt{\frac{K_{\text{eff}}}{M_{\text{eff}}}} = \sqrt{\int_0^1 \frac{EI}{L^3}\left(\frac{\partial^2\phi}{\partial\tau^2}\right)^2 \mathrm{d}\tau \Big/ \int_0^1 \rho AL\phi^2 \,\mathrm{d}\tau} = \left(\frac{4.730}{L}\right)^2\sqrt{\frac{EI}{\rho A}}. \tag{6}$$

2.2. Forced vibration

In order to keep the resonant beam vibrating at its frequency, the driving force is necessary. The resonant beam is excited by an oscillator, and vibrates at its resonant frequency. For each vibration mode, the input of the drive oscillator is connected to the detection devices, and its output is connected to the driving devices. The periodic axial force will cause axial push and pull loading on the resonant beam to shift its resonant frequency. As a result, the frequency shift of the resonant beam is a function of the applied periodic axial force, which could be utilized to sense the pressure, acceleration, or angular velocity. Figure 2 shows the operating principle of the resonant beam.

When applying driving force F_{d}, the resonant beam works at its resonant frequency, and the dynamic equation could be described as

$$\int_0^L \rho A\phi^2 \,\mathrm{d}x\ddot{q} + \int_0^L \xi\phi^2 \,\mathrm{d}x\dot{q} + \left(\int_0^L EI\left(\frac{\partial^2\phi}{\partial x^2}\right)^2 \mathrm{d}x + \int_0^L F\left(\frac{\partial\phi}{\partial x}\right)^2 \mathrm{d}x\right)q = F_{\text{d}}. \tag{7}$$

The function of driving forceF_{d} keeps the resonant beam working at resonant frequency. Therefore, we have

$$\int_0^L \xi\phi^2 \,\mathrm{d}x\dot{q} = F_{\text{d}}, \tag{8}$$

$$\ddot{q}(t) + \omega_0^2\left(1 + \frac{0.293L^3F_0\cos\omega_{\text{d}}t}{EI}\right)q(t) = 0. \tag{9}$$

If the transformations are chosen properly, Eq. (9) can be transformed to a standard form. Let $\delta' = \omega_0^2$ and

$\varepsilon' = 0.293L^3F_0\omega_0^2/EI$, it may be written as

$$\ddot{q}(t) + (\delta' + \varepsilon' \cos \omega_{\rm d} t)\, q(t) = 0. \tag{10}$$

In order to perform the method of small parameter perturbation, the differential equation (9) must be transformed to a standard form in parametric resonance. Assuming

$$\begin{aligned} z &= \frac{\omega_{\rm d} t}{2}, \quad q'' = \frac{{\rm d}^2 q}{{\rm d}z^2}, \\ S &= \frac{0.293L^3}{2EI}\delta = \delta' \left(\frac{2}{\omega_{\rm d}}\right)^2 = 4\left(\frac{\omega_0}{\omega_{\rm d}}\right)^2, \\ \varepsilon &= 2\varepsilon' \left(\frac{2}{\omega_{\rm d}}\right)^2 = 4\left(\frac{\omega_0}{\omega_{\rm d}}\right)^2 \frac{0.293L^3F_0}{2EI} \\ &= 4\left(\frac{\omega_0}{\omega_{\rm d}}\right)^2 SF_0, \end{aligned}$$

Equation (10) becomes Eq. (1)

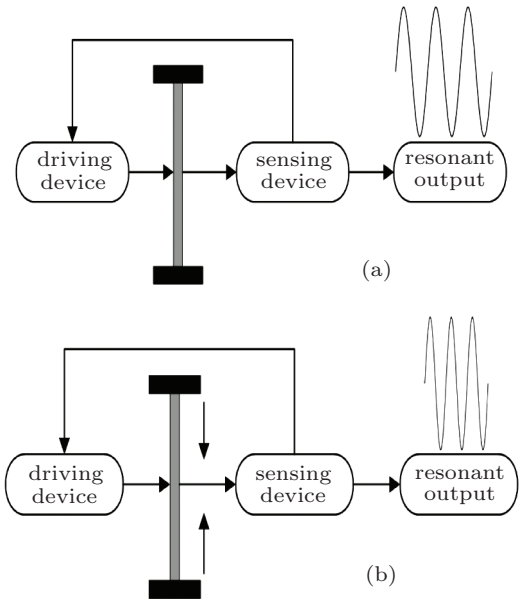


Fig. 2. Schematic diagram of the operating principle of the resonant beam. (a) No loading. (b) Compressed loading.

Equation (1) is known as the standard Mathieu equation. From Eq. (1), the resonant beam vibration stiffness $k = \delta + \varepsilon \cos 2z$ changes with the periodic axial force applied on the resonant beam, which makes the resonant frequency of the resonant beam change. The parameter δ represents the natural resonant frequency of the resonant beam The significant perturbation term $\varepsilon \cos 2z$ represents the modulation of the stiffness of the resonant beam at the periodic axial force frequency $\omega_{\rm d}$.

3. Parametric stability analysis

The results in Section 2 are derived without any additional damping in the mechanical model. Consequently, the algebraic expressions are not completed and optimal to analyze the stability in resonant beam. Actually, the resonant beam does not always work at the resonant state, and the driving force does not exactly counteract weak damping, so the dynamic equation is perhaps Eq. (2) known as the weakly damped Mathieu equation. Equation (2) exactly describes the parametric excitement dynamic characteristic of the resonant beams. This equation has been widely studied in the context of parametric resonance, and the approximate solution of the Mathieu equation may be either bounded or unbounded, which is dependent on the parameters in the equation. Hence, it is of interest to characterize the dynamic stability of resonant beams by analyzing the stability of a weakly damped Mathieu equation.

3.1. Stability criterion

We aiming at determining a stability condition for Eq. (2). Michael[34] has shown that for large δ and small μ, the stability criterion is assured if $|\varepsilon| < 2\mu$. In this paper, an improved stability criterion is obtained using periodic Lyapunov functions.[35]

Let $q = q_1$ and $\dot{q} = q_2$, Eq. (2) can be rewritten as

$$q_1' = q_2, \tag{11}$$

$$q_2' = -\mu q_2 - (\delta + \varepsilon \cos 2z)\, q_1. \tag{12}$$

Consider the Lyapunov function

$$V_1 = (\delta + k\mu + k\varepsilon \sin 2z)\, q_1^2 + 2kq_1q_2 + q_2^2, \tag{13}$$

where k is a parameter to be chosen. Differentiating Eq. (13) with respect to time and using Eqs. (11) and (12), then we obtain

$$\begin{aligned} V_1' = {} & -2k\delta q_1^2 - 2\varepsilon\,(\cos 2z - k \sin 2z)\, q_1 q_2 \\ & - 2\,(k - \mu)\, q_2^2. \end{aligned} \tag{14}$$

If V_1' is negative definite and $0 < \varepsilon \leq \delta$, we require

$$0 < k < \mu, \tag{15}$$

and

$$\varepsilon^2 < \frac{4k\delta(\mu - k)}{(1 + k^2)}. \tag{16}$$

Now we choose the value of k as

$$k = \frac{\sqrt{\mu^2+1}-1}{\mu}, \tag{17}$$

which maximizes the right-hand side of Eq. (16) and also satisfies Eq. (15). It can be easily proved that, for the above value of k, the function V_1 is positive definite. Substituting Eq. (17) into Eq. (16) yields the stability criterion as

$$|\varepsilon| < \sqrt{2\delta}\sqrt{\sqrt{\mu^2+1}-1} = \beta_1. \tag{18}$$

Now consider another Lyapunov function given by

$$V_2 = (\delta + \varepsilon\cos 2z)\, q_1^2 + (\mu q_1 + q_2)^2. \tag{19}$$

Differentiating Eq. (19) and using Eqs. (11) and (12), we have

$$\dot{V}_2 = -\left[2\mu\delta + 2\mu\varepsilon\cos 2z + 2\varepsilon\sin 2z\right] q_1^2. \tag{20}$$

We see that V_2' can only be negative semidefinite since $V_2' \equiv 0$ when $q_1 \equiv 0$. It can be easily seen that when $q_1 \equiv 0$, q_2 is also identically zero. Hence, if $\dot{V}_2$ is negative semi-definite, it is required that

$$|\varepsilon| < \frac{\mu\delta}{\sqrt{\mu^2+1}} = \beta_2. \tag{21}$$

Combining Eq. (18) and Eq. (21), the stability criterion can be written as

$$|\varepsilon| < \min\left[\sqrt{2\delta}\sqrt{\sqrt{\mu^2+1}-1}, \frac{\mu\delta}{\sqrt{\mu^2+1}}\right] = \beta. \tag{22}$$

3.2. Stability regions

For the resonant beams, with limitation of parameters δ and ε, its stable regions could be achieved by using the small parameter perturbation method.[12] In Eq. (2), the period $T = \pi$ and ε can be naturally assumed to be small. The solution $q(z,\varepsilon)$ and $\delta(\varepsilon)$ can be expanded into a series of powers of ε as follows:

$$\begin{cases} q = q_0(z) + \varepsilon q_1(z) + \varepsilon^2 q_2(z) + \cdots \\ \delta = \delta_0 + \varepsilon\delta_1 + \varepsilon^2\delta_2 + \cdots \end{cases} \tag{23}$$

Substituting Eq. (23) into Eq. (2) and gathering terms of the same order with respect to ε can obtain the following differential equations:

$$\begin{cases} q_0'' + \mu q_0' + \delta_0 q_0 = 0, \\ q_1'' + \mu q_1' + \delta_0 q_1 + \delta_1 q_0 = -q_0\cos 2z, \\ q_2'' + \mu q_2' + \delta_0 q_2 + \delta_1 q_1 + \delta_2 q_0 = -q_1\cos 2z. \end{cases} \tag{24}$$

In addition, each function $q(z)$ should have the period $T = \pi$. Therefore, the first identity of Eq. (24) leads to the following values for δ_0:

$$\delta_0 = \left(\frac{\pi n}{T}\right)^2 = n^2, \quad (n = 0, 1, \ldots), \tag{25}$$

and the following functions for q_0:

$$q_0 = a\cos\sqrt{\delta_0}z + b\sin\sqrt{\delta_0}z = a\cos nz + b\sin nz, \quad (n = 0, 1, \ldots), \tag{26}$$

where $q(0) = a$ and $q'(0) = b$.

We proceed to the higher order for the different values of n ($n = 0, 1, \ldots$), using the result from the Floquet theory. Then substituting the power series (26) into Eq. (24), we have

$$\begin{cases} \delta = -\dfrac{1}{8}\varepsilon^2 + o(\varepsilon^3), \\ \delta = 1 \pm \sqrt{\dfrac{1}{4}\varepsilon^2 - \mu^2} - \dfrac{1}{32}\varepsilon^2 + o(\varepsilon^3), \\ \delta = 4 + \dfrac{5}{48}\varepsilon^2 \pm \sqrt{\dfrac{\varepsilon^4}{256} - 4\mu^2} + o(\varepsilon^3), \\ \cdots \end{cases} \tag{27}$$

These equations with δ and ε furnish approximations to the transition values of ε and δ. In this way the stable regions of the weakly damped Mathieu equation have been completely determined The result of the perturbation expansion to the second order leads to an approximation of the boundary curves for a non-damped Mathieu equation ($\mu = 0$), which are shown in Fig. 3. Unstable regions are shaded. Boundaries are stable.

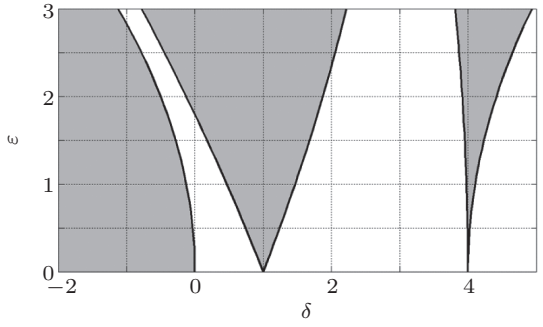


Fig. 3. Stability diagram of the Mathieu equation for small ε with $\mu = 0$.

The dynamic stability of the resonant beams based on the Mathieu equation is just theoretical analysis, which will be evaluated by simulation and discussion in the next section.

4. Numerical results and discussion

To validate the stability of the beam model, various numerical results are evaluated and compared with available beam parameters. As can be seen from Table 1, the Euler-Bernoulli clamped-clamped beam with properties is considered for the dynamic stability analysis.

Table 1. The parameters of the Euler–Bernoulli clamped–clamped beam. ρ: density, E: Young's modulus; L: beam length; I: area moment of inertia of the beam; F_0: axial force; ω_0: natural resonant frequency of the beam; $\omega_{\rm d}$: excitation frequency of the periodic axial force.

Parameter	Value
$\rho/(\mathrm{kg/m^3})$	7.8×10^3
E/Pa	2×10^{11}
L/m	0.03
$I/\mathrm{m^4}$	6.7500×10^{-15}
F_0/N	1
ω_0/Hz	1.7350×10^3
$\omega_{\rm d}$/Hz	30

First, the value of the damped coefficient is defined as $\mu = 0.1$. Only δ and μ appear in the stability criterion, and the value of δ is dependent on material properties and geometric dimensioning. As can be seen from Fig. 4, in despite of the value of δ, β_2 is always greater than β_1. Secondly, it is assumed in the computation that the beam length $L = 30$ mm, so the parameter $\delta = 1.3379 \times 10^4$ is determined. As can be seen from Fig. 5, despite of the value of μ, β_2 is always greater than β_1. From the comparison between Fig. 4 and Fig. 5, it is found that no matter how the parameters δ and μ change, β_2 is always greater than β_1. Therefore, $\varepsilon < \beta_1$ is enough to satisfy the stability criterion, which is shown in Eq. (22).

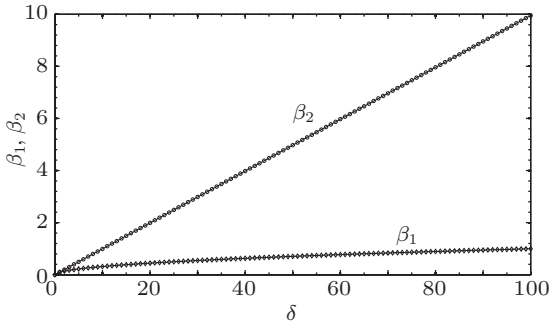


Fig. 4. Comparison between β_1 and β_2 with $\mu = 0.1$.

Figure 6 shows the comparison between ε and β_1, when resonant beams have different lengths ($L = 30$, 40, 50, 60, and 70 mm), the damped coefficient $\mu = 0.1$, and the axial force $F_0 = 1$ N. Please note that ε is the ratio between the natural resonant frequency of the beam and the excitation frequency of the periodic axial force. Hence, ε is independent of the beam length. As shown in Fig. 6, as special cases, beam length $L = 50$, 60, and 70 mm implies that the beam is not in the status of stability under all the conditions according to the stability criterion, since ε is not smaller than β_1. As another special case, beam length $L = 30$ and 40 mm implies that the beam is in the status of stability under all the conditions, since ε is always smaller than β_1. Therefore, the beam length $L = 30$ mm is reasonable.

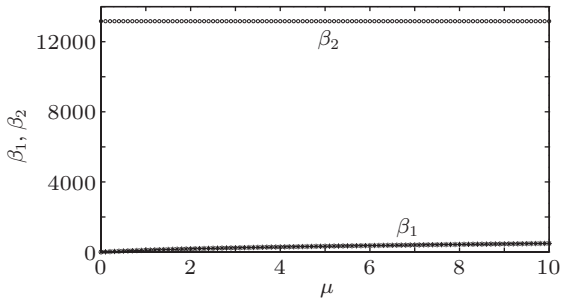


Fig. 5. Comparison between β_1 and β_2 with $\delta = 1.3379 \times 10^4$.

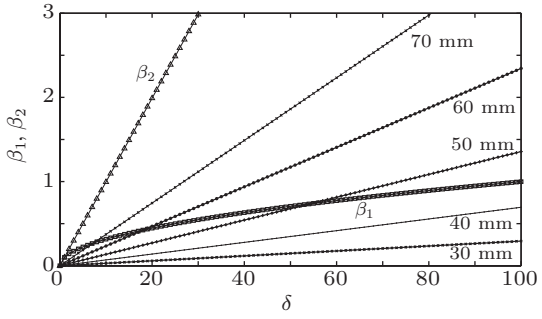


Fig. 6. Comparison between β_1 and ε with different beam lengths.

Figure 7 shows the comparison between ε and β_1, when resonant beams are subjected to axial compressive force $F_0 = 1$, 2, 3, 4, 5 N, and the damped coefficient value $\mu = 0.1$. A larger axial compressive force weakens the bending stiffness of the beam and consequently results in smaller frequencies. As shown in Fig. 7, it can be observed that beams have stronger stability when $F_0 = 1$, 2, and 3 N than $F_0 = 4$, 5 N beams due to their much stronger stiffness. As one special case, axial compressive force $F_0 = 4$, 5 N implies that the beam is not in the status of stability

under all the conditions according to the stability criterion, since ε is not smaller than β_1. As another special case, axial compressive force $F_0 = 1$, 2, and 3 N implies that the beam is stable under all the conditions, because ε is always smaller than β_1. Therefore, axial compressive force $F_0 = 1$ N is reasonable.

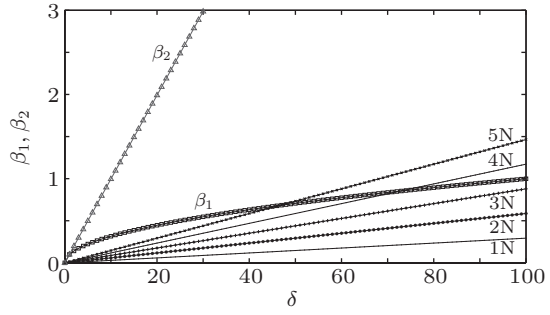


Fig. 7. Comparison between β_1 and ε with different axial forces.

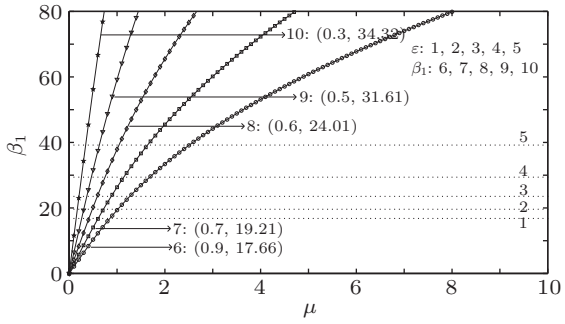


Fig. 8. Comparison between β_1 and ε with different beam lengths.

Figure 8 shows the effect of the damped coefficient on the stability of resonant beams by comparing the stability curves of resonant beams with different beam lengths. Table 2 gives the computation parameters used in this example. In order to examine the influences of the damped coefficient, the beam is subjected to the axial compressive force $F_0 = 1$ N. Among the five beam lengths considered, the condition of the damped coefficient is the highest for $L = 30$ mm and lowest for $L = 70$ mm. The stability conditions about the damped coefficient and beam length are shown in Table 2. The damped coefficient should reach its lowest value $\mu = 0.9$ when the beam length L is 30 mm.

Table 2. The parameters ε and β_1 for different resonant beam lengths, and the stable condition of the damped coefficient.

Beam length	ε	β_1	Stability condition
$L = 30$ mm	1	6	$\mu > 0.9$
$L = 40$ mm	2	7	$\mu > 0.7$
$L = 50$ mm	3	8	$\mu > 0.6$
$L = 60$ mm	4	9	$\mu > 0.5$
$L = 70$ mm	5	10	$\mu > 0.3$

Figure 9 presents the stability regions of resonant beams with different damped coefficients. The instability regions move further to the underside and become much narrower as the damped coefficient increases. Hence the damped coefficient acting on the beam, which plays an important role on the beam stability, is shown in Fig. 9. Table 3 presents the contrast to beam parameters (δ and ε) between theoretical and stability regions corresponding to the first parameters of different beam lengths ($F_0 = 1$ N, $\omega_d = 30$ Hz). It can be seen that the theoretical points are much lower than the stability boundary points, according to the stability regions of Figs. 3, 8, and 9. The parameters of the beam are reasonable to keep the beam in its stable states.

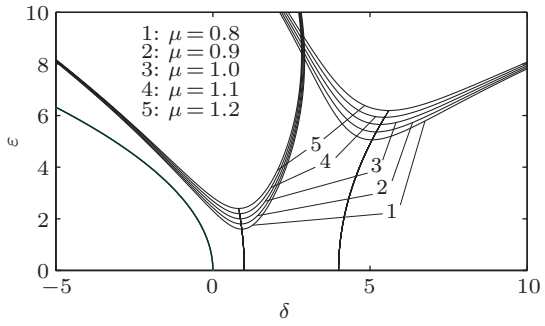


Fig. 9. Stability diagram of the Mathieu equation with different damped coefficients.

Table 3. Comparison of the theoretical and simulated values of the resonant beam stable point.

Beam length	Symbol	Theory point	Stability boundary point
$L = 30$ mm	(δ, ε)	(1.3379×10^4, 39.1996)	(1.3379×10^4, 8.9499×10^3)
$L = 40$ mm	(δ, ε)	(4.2331×10^3, 29.3997)	(4.2331×10^3, 2.2475×10^3)
$L = 50$ mm	(δ, ε)	(1.7339×10^3, 23.5198)	(1.7339×10^3, 892.0737)
$L = 60$ mm	(δ, ε)	(836.1688, 19.5998)	(836.1688, 373.9461)
$L = 70$ mm	(δ, ε)	(451.3431, 16.7998)	(451.3431, 167.6246)

5. Conclusion

The dynamic behavior of a resonant beam subjected to periodic axial force has been examined and discussed. Based on our results in this work, we arrive at several conclusions.

i) The dynamic characteristic of the resonant beams with periodic axial force is equivalent to a parametric resonant system which could be described by the Mathieu equation.

ii) An improved stability criterion is obtained using periodic Lyapunov functions. An approximate analysis based on the small parameter perturbation method has been employed to investigate the stability regions of the Mathieu equation.

iii) No matter how the parameters δ and μ change, β_2 is always greater than β_1 Hence, $\varepsilon < \beta_1$ is enough to satisfy the stability criterion.

iv) In order to keep the beam stable, when the beam length decreases, the conditions of the damped coefficient rise instead.

v) The unstable regions move to the underside and become much narrower as the damped coefficient increases.

vi) Numerical results show that the beam parameters we choose comply with the stability criterion and condition.

References

[1] Seshia A A 2002 *Integrated Micromechanical Resonant Sensors for Inertial Measurement Systems* (Ph.D. Thesis) (University of California, Berkeley)

[2] Yang J B, Jiang L J and Chen D C 2004 *J. Sound Vib.* **274** 863

[3] Jeong C, Seok S, Lee B, Kim H and Chun K 2004 *J. Micromech. Microeng* **14** 1530

[4] Mahmoodi S N, Jalili N and Khadem S E 2008 *J. Sound Vib.* **311** 1409

[5] Zhang J H, Mao X L and Liu Q Q 2012 *Chin. Phys.* B **21** 86101

[6] Li S S, Lan J and Han B 2012 *Chin. Phys.* B **21** 064601

[7] Prak A1993 *Silicon Resonant Sensors: Operation and Response* (Ph.D. Thesis) (Netherlands: University of Twente)

[8] Roessig T A 1998 *Integrated MEMS Tuning Fork Oscillators for Sensor Applications* (Ph.D. Thesis) (University of California, Berkeley)

[9] Tabata O and Yamamoto T 1999 *Sensor. Actuat.* A-*Phys.* **75** 53

[10] Bilic D, Howe R T, Clark W A and Roessig T A 1999 *The 10th International Conference on Solid-State Sensors and Actuators*, *Transducers* Sendai, Japan, p. 1824

[11] Recktenward G and Rand R 2005 *Int. J. Nonlinear Mech.* **40** 1160

[12] McLachlan N W 1964 *Theory and Application of Mathieu Function* (Dover Publicatons Inc)

[13] Harris C and Crede C 1976 *Shock and Vibration Handbook* (2nd ed.) (Mc-Graw Hill) pp. 1–13

[14] Liu S S and Liu S D 2002 *Special Function* (Weather Publicatons Inc) pp. 737–739 (in Chinese)

[15] Wang Y Z and Zhou Y Z 2011 *Chin. Phys.* B **20** 040501

[16] Fan S C and Li Y 2011 *Chin. Phys.* B **21** 050401

[17] Francis J P and Glenn R F 2008 *Proc. R. Soc.* A **464** 1885

[18] Coisson R, Vernizzi G and Yang X K *International Workshop on Open-source Software for Scientific Computation* (Chap. 3), September 18–20 2009 Guiyang, China, p. 1

[19] Rand R H, Sah S M and Suchorsky M K 2010 *Commun. Nonlinear Sci. Numer. Simulat.* **15** 3254

[20] Arrowsmith D Kand Mondragon R J 1999 *Meccanica.* **34** 401

[21] Younesian D, Esmailzadeh E and Sedaghati R 2005 *Nonlinear Dyn.* **39** 335

[22] Guennoun K, Houssni M and Belhaq M 2002 *Nonlinear Dyn.* **27** 211

[23] Susan, Wooden M and Sinha S C 2007 *Nonlinear Dyn.* **47** 263

[24] Thomas and Waters J 2010 *Nonlinear Dyn.* **60** 341

[25] Zounes R S and Rand R H 2002 *Nonlinear Dyn.* **27** 87

[26] Belhap M, Guennoun K and Houssni M 2002 *Int. J. Nonlinear Mech.* **37** 445

[27] Maharana P K and Shrivastava S K 1984 *Acta Astronautica.* **11** 103

[28] Taylor J H and Narendra K S 1969 *SIAM J Appl. Math.* **17** 343

[29] Gunderson H, Rigas H and Van Vleck F S 1974 *SIAM J Appl. Math.* **26** 345

[30] Pipes L A 1953 *J. Appl. Phys.* **24** 902

[31] Richards J A 1976 *Appl. Math.* **30** 240

[32] Richards J A 1977 *Proc. IEEE* **65** 1549

[33] Richards J A 1983 *Analysis of Periodically Time Varying Systems* (New York: Springer Verlag)

[34] Michael G J 1967 *IEEE Trans. Automat. Contr.* **12** 337

[35] Ramarajan S and Rao S N 1971 *IEEE Trans. Automat. Contr.* **67** 363